Cell

Role of the Clathrin Terminal Domain in Regulating Coated Pit Dynamics Revealed by Small Molecule Inhibition

Lisa von Kleist,[1] Wiebke Stahlschmidt,[1] Haydar Bulut,[1,8] Kira Gromova,[1,8] Dmytro Puchkov,[1,8] Mark J. Robertson,[2] Kylie A. MacGregor,[2] Nikolay Tomilin,[3] Arndt Pechstein,[1,3] Ngoc Chau,[4] Megan Chircop,[4] Jennette Sakoff,[5] Jens Peter von Kries,[6] Wolfram Saenger,[1] Hans-Georg Kräusslich,[7] Oleg Shupliakov,[3] Phillip J. Robinson,[4] Adam McCluskey,[2] and Volker Haucke[1,6,*]

[1]Institute of Chemistry and Biochemistry & Neurocure Cluster of Excellence, Freie Universität Berlin, 14195 Berlin, Germany
[2]Centre for Chemical Biology, Chemistry, The University of Newcastle, Callaghan NSW 2308, Australia
[3]Department of Neuroscience, DBRM, Karolinska Institutet, 17117 Stockholm, Sweden
[4]Cell Signalling Unit, Children's Medical Research Institute, The University of Sydney, Sydney NSW 2145, Australia
[5]Department of Medical Oncology, Calvary Mater Newcastle Hospital, Waratah NSW 2298, Australia
[6]Leibniz-Institut für Molekulare Pharmakologie (FMP), 13125 Berlin-Buch, Germany
[7]Department of Infectious Diseases, Virology, University of Heidelberg, 69120 Heidelberg, Germany
[8]These authors contributed equally to this work
*Correspondence: volker.haucke@fu-berlin.de
DOI 10.1016/j.cell.2011.06.025

SUMMARY

Clathrin-mediated endocytosis (CME) regulates many cell physiological processes such as the internalization of growth factors and receptors, entry of pathogens, and synaptic transmission. Within the endocytic network, clathrin functions as a central organizing platform for coated pit assembly and dissociation via its terminal domain (TD). We report the design and synthesis of two compounds named pitstops that selectively block endocytic ligand association with the clathrin TD as confirmed by X-ray crystallography. Pitstop-induced inhibition of clathrin TD function acutely interferes with receptor-mediated endocytosis, entry of HIV, and synaptic vesicle recycling. Endocytosis inhibition is caused by a dramatic increase in the lifetimes of clathrin coat components, including FCHo, clathrin, and dynamin, suggesting that the clathrin TD regulates coated pit dynamics. Pitstops provide new tools to address clathrin function in cell physiology with potential applications as inhibitors of virus and pathogen entry and as modulators of cell signaling.

INTRODUCTION

Clathrin-mediated endocytosis (CME) regulates the cell surface levels and endocytic uptake of important plasma membrane proteins (Brodsky et al., 2001; Conner and Schmid, 2003). These include nutrient and growth factor receptors, ion channels, adhesion proteins, and synaptic vesicle (SV) proteins in the brain. The clathrin-based endocytic machinery is also hijacked by pathogens such as bacteria and viruses to get access to the cell interior (Conner and Schmid, 2003; Miyauchi et al., 2009; Veiga et al., 2007). Assembly of clathrin-coated pits (CCPs) likely is initiated by the recruitment of early-acting endocytic proteins such as FCHo 1/2, intersectins, and Eps15/Eps15R (Henne et al., 2010; Pechstein et al., 2010). These factors serve as scaffolds for the coassembly of AP-2, which coordinates recognition of transmembrane cargo (Edeling et al., 2006) with recruitment of accessory proteins. Early endocytic structures are stabilized by an assembling clathrin coat built from soluble clathrin triskelia comprising three heavy and three light chains (Brodsky et al., 2001; Conner and Schmid, 2003; Edeling et al., 2006). The central building block of triskelia is the 190 kDa clathrin heavy chain, which forms an extended three-legged structure. The N-terminal β-propeller domain (TD) at the distal end of the leg adopts a WD40-like fold (ter Haar et al., 2000), while the C terminus is near the vertex of the triskelion (Brodsky et al., 2001).

The clathrin cage has been postulated to serve at least two major functions in endocytosis: (1) stabilizing deformed membrane domains (Hinrichsen et al., 2006) and (2) providing an interaction hub for the recruitment of accessory factors that regulate progression of endocytosis (Schmid and McMahon, 2007). Structural and proteomic studies have revealed a surprisingly simple architecture of accessory protein-clathrin interactions (Schmid and McMahon, 2007). Most of these factors, including amphiphysins, AP180, and SNX9, harbor so-called clathrin box motifs (or variants thereof), simple degenerate peptides that bind to a structurally well-defined site on the TD of clathrin heavy chain (ter Haar et al., 2000). Consistent with the proposed function of the TD as a central protein-protein interaction hub (Schmid and McMahon, 2007) overexpression of clathrin-binding fragments of endocytic proteins causes the sequestration of clathrin within the cytoplasm (Slepnev et al., 2000), suggesting that multiple redundant interactions of accessory proteins with the TD serve to recruit clathrin to membranes. However, overexpression experiments need to be interpreted

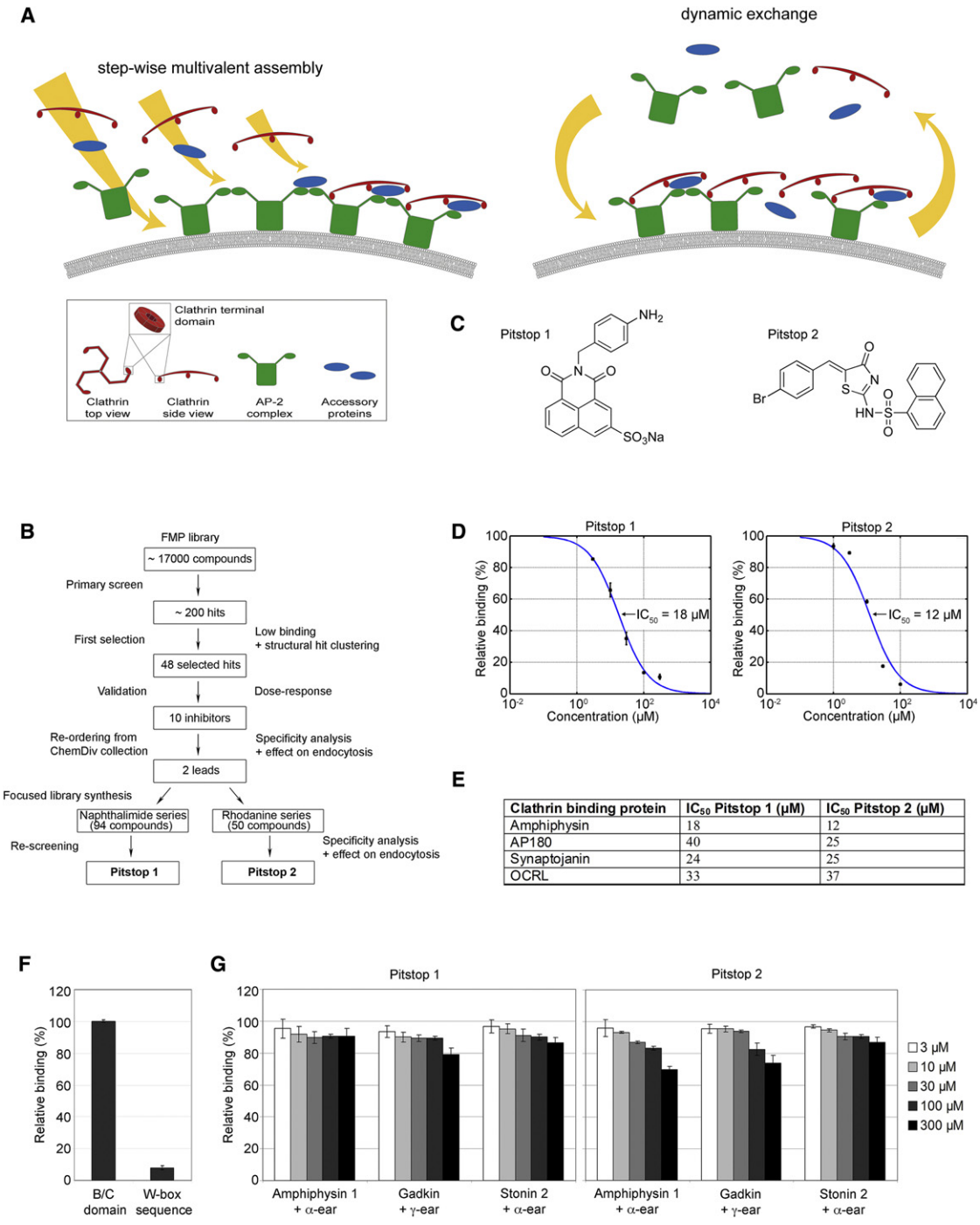

Clathrin binding protein	IC_{50} Pitstop 1 (μM)	IC_{50} Pitstop 2 (μM)
Amphiphysin	18	12
AP180	40	25
Synaptojanin	24	25
OCRL	33	37

Figure 1. Pitstops Selectively Inhibit Ligand Association with the Clathrin Terminal Domain

(A) Hypothetical models depicting the potential roles of clathrin TD-ligand association in endocytosis. Multiple redundant interactions of the clathrin TD with its endocytic ligands (blue) may serve to stably recruit clathrin to membranes, thereby facilitating assembly through local enrichment (left). Alternatively, clathrin assembled at endocytic sites could serve as an organizing scaffold that regulates CCP dynamics by providing spatially defined binding sites on its TD for accessory proteins that drive CCP maturation and disassembly (right).

(B) Schematic diagram outlining the compound screening strategy.

(C) Chemical structures of pitstops 1 and 2.

(D) Dose dependence of pitstop-mediated interference with clathrin TD-amphiphysin B/C complex formation. Values from ELISA were normalized to solvent controls (set to 100%). Data represent SEM (n = 3 independent experiments).

(E) IC_{50} values of pitstop-mediated interference with clathrin TD complex formation determined by ELISA. AP180, C-terminal domain of AP180; Synaptojanin, C-terminal domain of synaptojanin 1-p170; OCRL, PH domain of OCRL. Data represent SEM (n = 3 independent experiments).

with caution as evidenced by the comparably mild phenotypes of clathrin-binding accessory protein knockdowns or knockouts in mice (Dittman and Ryan, 2009; Mettlen et al., 2009). Moreover, dominant-negative and genetic approaches bear the inherent disadvantage that indirect effects caused by sustained expression or loss-of-function cannot be distinguished from direct phenotypes. It is thus essential to identify molecular reagents that can selectively and acutely interfere with CME. No specific compounds targeting clathrin are available so far.

Here, we describe the identification and characterization of two small molecule inhibitors of clathrin TD function, named pitstops for their ability to stall clathrin-coated pit (CCP) dynamics, which acutely interfere with receptor-mediated endocytosis, entry of HIV, and SV reformation. Pitstops provide tools to address clathrin function in cell physiology with potential applications as inhibitors of virus and pathogen entry and as modulators of cell signaling.

RESULTS

Pitstops Are Nontoxic Specific Inhibitors of Endocytic Ligand Association with the Clathrin Terminal Domain

Clathrin function in mammalian cells has been addressed mainly via knockdown (Motley et al., 2003) or dominant-negative approaches (Dittman and Ryan, 2009; Slepnev et al., 2000). At invertebrate neuromuscular junctions using transgenic flies clathrin has also been targeted by photoinactivation (Heerssen et al., 2008). While these strategies have shown that clathrin is essential for CCP formation or stability, no information exists regarding the physiological role of endocytic ligand association of its TD. This is a surprising knowledge gap given the fact that clathrin box-TD interactions form a major hub within the endocytic network (Schmid and McMahon, 2007). Based on previous cell biological and biochemical studies, it was suggested that multiple redundant interactions of the clathrin TD with its endocytic ligands may serve to stably recruit clathrin to membranes, thereby facilitating clathrin assembly through local enrichment (Figure 1A, left). Alternatively, clathrin assembled at nascent endocytic sites could serve as an organizing scaffold that regulates CCP dynamics by providing spatially defined binding sites on its TD for accessory proteins that drive CCP maturation and disassembly (Figure 1A, right).

To distinguish between these models, we used a chemical biology approach designed to identify inhibitors of complex formation between the TD and its endocytic ligands. We carried out an ELISA-based screen for small molecules that can interfere with clathrin TD association of the B/C domain of amphiphysin, an endocytic protein harboring a clathrin box motif (Slepnev et al., 2000). Screening a library of about 17,000 small molecules from the central open access technology platform of the ChemBioNet, we identified and validated (see Extended Experimental Procedures available online) two lead compounds that exhibited selective inhibition of clathrin TD-amphiphysin association (Figure 1B). Retrosynthetic analysis identified simple approaches to in-house synthesis of two focused compound libraries based on the original leads. This led to the identification of two molecules of distinct chemical scaffolds, which specifically disrupt ligand association with the clathrin TD. Based on subsequent studies and their ability to impair CCP function (see below) we named these compounds pitstops 1 (from the naphthalimide library) and 2 (from the rhodanine library, Figure 1C). Pitstops 1 and 2 selectively inhibited amphiphysin association of clathrin TD with IC_{50} values of 18 and 12 μM, respectively (Figure 1D). Consistent with a crucial role for the clathrin box within amphiphysin for clathrin TD association a truncation mutant lacking the clathrin box sequence displayed a near complete loss of its clathrin TD binding ability (Figure 1F), similar to that seen in pitstop-treated samples. Clathrin TD binding of other endocytic proteins such as the C-terminal domains of AP180 and synaptojanin 1 (p170), or the PH domain of OCRL was also inhibited with IC_{50}s between 24 and 40 μM (Figure 1E). By contrast, neither compound affected complex formation between the ear domain of AP-2α and amphiphysin (a top-site ligand) or stonin 2 (a side-site ligand), or between the AP-1 γ-ear and its accessory binding partner gadkin (Figure 1G). Pitstops also did not influence the in vitro GTPase activity of full-length native sheep brain dynamin 1 (data not shown). Pitstops did not exhibit generalized cytotoxicity after 8 hr exposure in HeLa cells assayed by LDH activity (Figure S1A) or TUNEL staining to detect apoptotic cells (Figure S1B). Prolonged exposure (20 hr) to pitstops did not affect cell membrane integrity (Figures S1C and S1D) or induce apoptotic cell death (Figure S1E). Even longer exposure (72 hr) did not affect cell viability and proliferation in a variety of cell lines (Table S1). We conclude that pitstops act as selective inhibitors of clathrin TD function that do not adversely affect cell viability.

Pitstop Association with the Clathrin Terminal Domain Obstructs Binding of Clathrin Box Ligands

To understand the molecular basis of clathrin TD inhibition by pitstops, we determined the structure of the clathrin TD in complex with pitstops by protein X-ray crystallography. Clathrin TD-containing crystals diffracted up to a resolution of 1.7 Å and the structure was solved by molecular replacement using the clathrin TD as a search model (Table S2). Following refinement, inhibitor molecules in complex with clathrin TD could be identified and modeled into the electron densities (Figures S2A and S2B). The overall structures of clathrin TD in complex with either pitstops 1 or 2 are shown in Figures 2A and 2C. The clathrin TD adopts a WD40-like structure comprised of a seven bladed β-propeller each with four antiparallel strands (ter Haar et al., 2000). Both inhibitors bind the interface between the first and second blades (Figures 2B and 2D) at a site largely overlapping with that used by clathrin box-containing accessory proteins (Figures 2E and 2F).

Pitstop 1 lies in a hydrophobic cavity formed by four isoleucines (52, 62, 80, 93), Leu82, and Phe91. Its conformation is stabilized by five hydrogen bonds at both ends of pitstop 1. Only one direct hydrogen bond is formed between the sulfonate

(F) Binding of amphiphysin 1 B/C (250-578) or a truncation lacking the clathrin box (365-578) to clathrin TD. Data represent SEM (n = 2) independent experiments.
(G) Pitstops do not affect other peptide-in-groove interactions in membrane traffic. Data represent SEM (n = 3 independent experiments).
See also Figure S1 and Table S1.

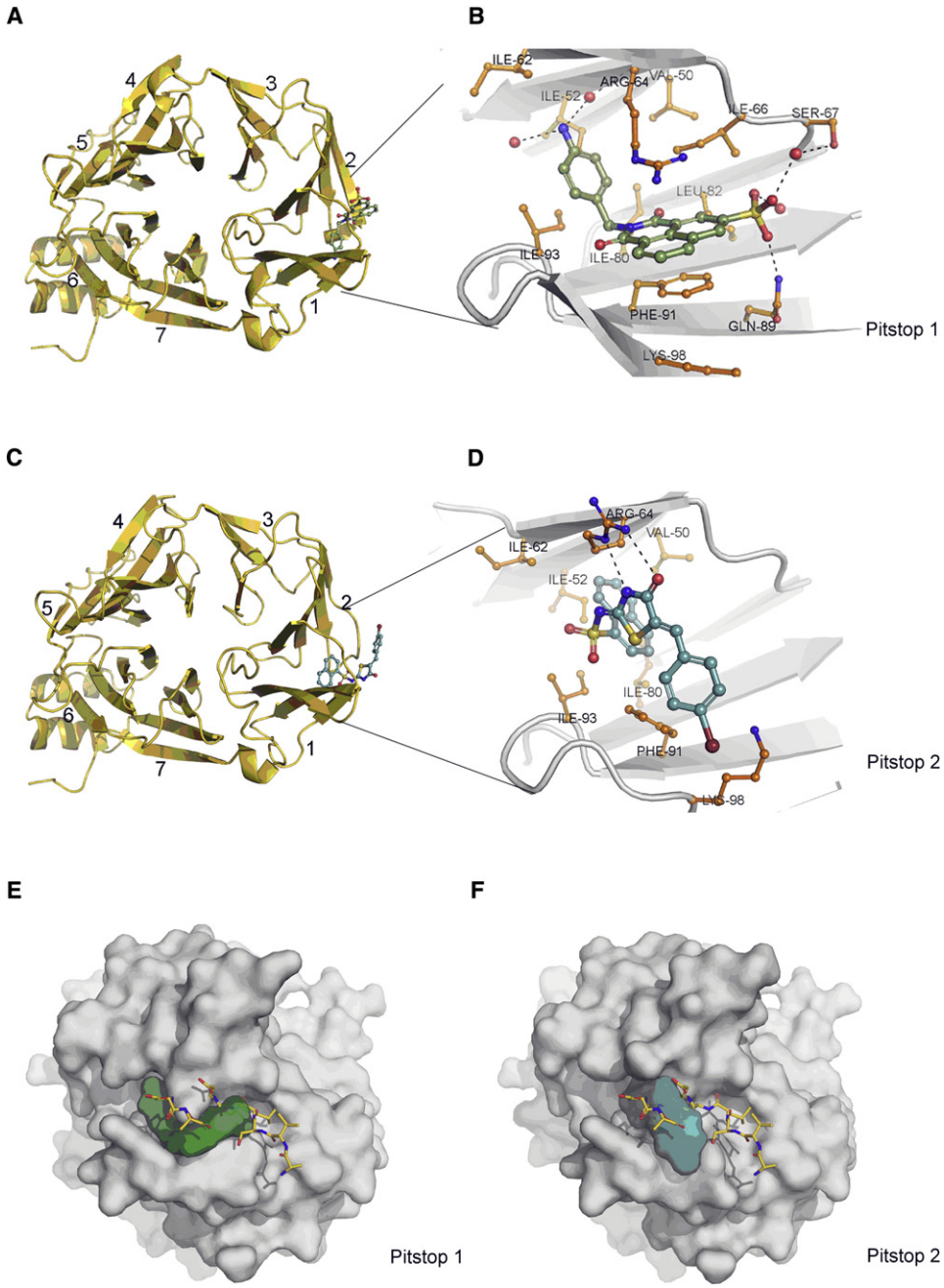

Figure 2. Pitstops Compete with Clathrin Box Ligands for a Common Site on the Clathrin TD

(A and C) Ribbon representations of the clathrin TD (top view). Blades of the TD-β-propeller are numbered from 1–7. Both inhibitors bind specifically to the clathrin-box binding site (between blades 1 and 2 of the clathrin TD).

(B) Close-up view of the binding site for pitstop 1. The inhibitor and amino acids of the binding groove are shown in ball-and-stick mode. Hydrogen bonds formed at both ends of pitstop 1 are indicated by broken lines. The nonpolar portion of pitstop 1 is sandwiched between Phe91 and the Arg64 side chains. On one side of the nonpolar portion of pitstop 1 parallel π-π stacking interactions take place with the aromatic ring of Phe91. On the other end polar π-stacking interactions take place between the guanidinium group of Arg64 (δ+ dipole) and the π-electrons of the aromatic rings (δ- dipole) of the inhibitor.

(D) Close-up view of the binding site for pitstop 2. The inhibitor and amino acids are shown in ball-and-stick mode. Bidentate hydrogen bonds at 3.0 Å distance are formed between the guanidinium group of Arg64 and O and N atoms of the central portion of pitstop 2. The aromatic ring of Phe91 is located in the same position as in the inhibitor-free form of the clathrin TD and stacks against the edge of the bromobenzene of pitstop 2.

(E and F) For comparison pitstops are superimposed with the clathrin box-containing AP-3 β3-hinge peptide (sequence AVSLLDLDA) highlighted with yellow sticks. Pitstop 1 is shown in green (left), pitstop 2 in blue (right), respectively.

See also Figure S2 and Table S2.

group of pitstop 1 and the ε-amino group (Nε2 atom) of Gln 89. All other hydrogen bonds are mediated by water (Figure 2B). Comparison of ligand-free clathrin TD with the pitstop 1-bound form shows that two residues in the clathrin box-binding site undergo major conformational changes upon ligand binding. While the phenyl ring of Phe 91 rotates by 60° around the Cα-Cβ bond and stacks against the nonpolar portion of the compound on one side, the guanidinium group of the Arg64 side-chain stacks on pitstop 1 on the opposite side (Figure S2C).

Pitstop 2 occupies the identical hydrophobic cavity used by pitstop 1. However, we also note significant differences in the binding modes of both molecules (Figure 2D). The side chain of Arg64 is positioned along the central part of pitstop 2 and forms bidentate hydrogen bonds with O and N atoms of the thiazol-4(5*H*)-one ring. The conformational change of Arg 64 allows enough space for the nonpolar portion of pitstop 2 to insert deeply into the hydrophobic cavity, toward the first blade. The phenyl ring of Phe 91 stacks against the nonpolar edge of the bromobenzene group of pitstop 2 (Figure 2D). Since the solvent-exposed bromobenzene moiety lies on the second blade of the clathrin TD, the first and the second blades are blocked by pitstop 2.

Our analysis reveals that two chemically unrelated pitstops fit into the targeted TD groove in two different poses and induce distinct structural changes in clathrin TD (Figure S2C). This provides a molecular basis for the selective displacement of clathrin box ligands from the TD and accounts for the in vitro and in vivo activities of pitstops.

Pitstop 2 Selectively Inhibits Clathrin-Mediated Endocytosis and HIV Entry

To examine whether pitstop 2 can act in living cells, we analyzed its effect on the internalization of transferrin (Tf) and epidermal growth factor (EGF), known ligands for CME (Conner and Schmid, 2003; Goh et al., 2010). When exposed to Alexa^{568}-Tf HeLa cells efficiently internalized Tf into perinuclear recycling endosomes. Preincubation of HeLa cells with pitstop 2 led to a dose-dependent inhibition of Tf uptake with an IC_{50} value (12–15 μM) very similar to that measured for blocking clathrin TD function in vitro (Figures 3A and 3B). Application of 30 μM pitstop 2 completely blocked Tf endocytosis, similar to what has been observed in clathrin knockdown cells (Motley et al., 2003). Pitstop 2-induced block of Tf endocytosis in HeLa cells was completely reversed within 1–3 hr of drug washout. In another cell line, U2OS, the IC_{50} for Tf uptake was 9.7 ± 1.5 μM (n = 5 independent experiments, three distinct synthetic batches). Treatment with similar concentrations of pitstop 2 also blocked Tf uptake in other cell types including Cos7 and BSC1 cells, astrocytes, or primary neurons (compare Figure S6). Pitstop 2 also caused a potent inhibition of EGF uptake (Figure 3C), consistent with the notion that the majority of EGF is endocytosed via a clathrin-mediated entry route in most cell types (Goh et al., 2010). Pitstop 1, which displays comparably low cell membrane penetration, exhibited qualitatively similar effects, albeit at much higher doses (data not shown).

To better understand the mechanism by which pitstop 2 inhibits receptor-mediated endocytosis, we incubated Cos7 cells with Alexa^{488}-EGF at 4°C to accumulate ligand-receptor complexes in CCPs. A similar, albeit slightly enhanced accumulation of EGF was observed in pitstop 2-treated cells (Figures 3D and 3E), suggesting that pitstop 2 does not interfere with cargo recognition or sequestration into CCPs, a step mediated by endocytic adaptors such as AP-2. These data argue against nonspecific effects of pitstop 2 on plasma membrane organization and suggests that pitstop 2 blocks CME at a step subsequent to cargo sequestration.

Shiga toxin is known to enter cells via a clathrin-independent glycosphingolipid-dependent route (Johannes and Römer, 2010). HeLa cells rapidly internalized Shiga toxin, which accumulated in the *cis*-Golgi area, irrespective of the presence of pitstop 2 (Figures 3F and 3G). We noticed a slight, though statistically insignificant delay, in Shiga toxin delivery to the *cis*-Golgi in pitstop 2-treated cells (Figure 3H), indicating that clathrin TD-ligand interactions are not required for retrograde transport of Shiga toxin, although they may facilitate its endosomal sorting (Saint-Pol et al., 2004). This supports the specificity of pitstop 2 for the CME pathway.

Many viruses and pathogens exploit the clathrin-dependent endocytic machinery for cell entry. HIV-1 entry into cells has recently been shown to occur predominantly or exclusively via CME in studies using dominant-negative dynamin or Eps15 (Daecke et al., 2005), or the small molecule dynamin inhibitor dynasore (Miyauchi et al., 2009). This suggests an obligatory role for clathrin in HIV-1 entry. To address this, we infected HeLa reporter cell lines for 2 hr with HIV-1 in the presence or absence of pitstop 2. Subsequent fusion events were blocked with an HIV entry inhibitor and infection was scored by luciferase readout. Pitstop 2 potently and specifically reduced HIV-1 infectivity by > 90% (Figure 3I and Figure S3F). A similar inhibition was seen if cytosolic HIV-1 entry was measured by quantifying virus-associated β-lactamase activity (Figure 3J) or by visualizing synthesis of the HIV structural protein p24 (Figure S3G). These data confirm that CME is the main route of productive HIV entry in this cell line.

Our results demonstrate that pitstop 2 is an efficient and selective inhibitor of CME that acts via blocking ligand access to the clathrin TD.

The Clathrin TD Plays a Crucial Role in Regulating Coated Pit Dynamics

Given the lack of knowledge regarding the physiological role of ligand binding to the clathrin TD in endocytosis, we chose to study clathrin dynamics in more detail. Live Cos7 cells stably expressing eGFP-clathrin light chains (LC) were monitored by total internal reflection microscopy (TIRFM). Consistent with previous data (Ehrlich et al., 2004) clathrin LC-containing CCPs formed and disappeared at the plasma membrane with most events exhibiting lifetimes between 26 and 89 s. A smaller fraction of long-lived clathrin-coated structures were detected with lifetimes of more than 90 s (Saffarian et al., 2009). Treatment of cells with pitstop 2 led to a dramatic shift toward long-lived clathrin-coated structures, many of which exhibiting lifetimes well beyond our usual imaging time (limited by the eventual bleaching of clathrin LC-eGFP) (Figures 4A and 4B). This is obvious from kymographs (Figure 4A) and from cumulative plots of CCP lifetimes (Figure 4C). Increased CCP lifetimes were paired with

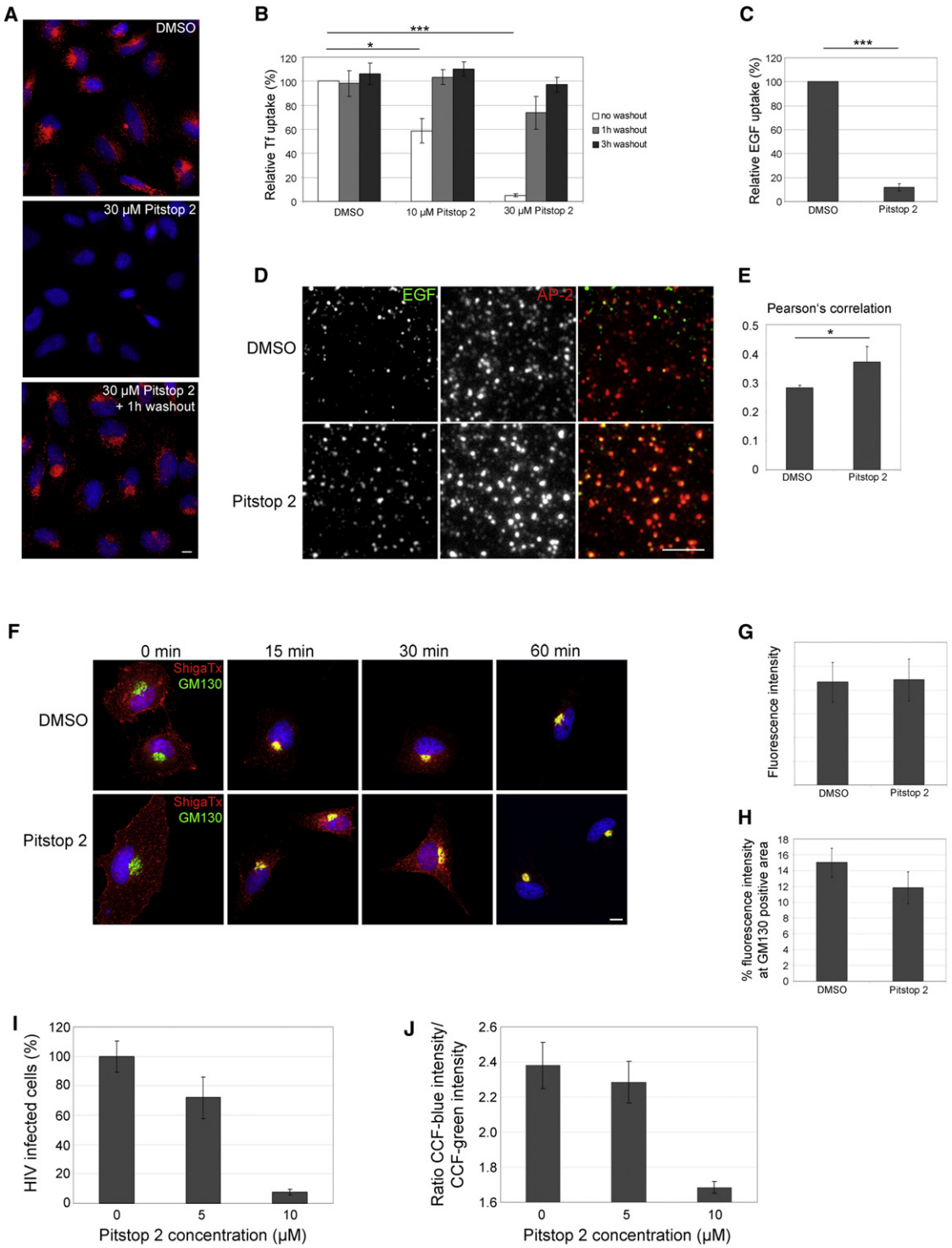

Figure 3. Pitstop 2 Reversibly Inhibits Clathrin-Mediated Endocytosis

(A) Pitstop 2 reversibly inhibits Tf uptake. After 15 min preincubation HeLa cells were incubated with Alexa^{568}-Tf in the presence of DMSO or 30 μM pitstop 2 for 15 min. Tf uptake is seen to resume after washout of the drug for 1 hr. Scale bar, 10 μm.

(B) Reversibility and dose dependence of pitstop 2-mediated inhibition of Tf uptake. Data represent SEM (n = 3 independent experiments; *$p < 0.05$, ***$p < 0.0001$).

(C) Pitstop 2 inhibits EGF uptake. HeLa cells pretreated with 30 μM pitstop 2 or DMSO for 15 min were incubated for 15 min with Alexa^{488}-EGF in the continued presence of inhibitor. Data represent SEM (n = 3 independent experiments; ***$p < 0.0001$).

(D) Pitstop 2 does not interfere with AP-2-mediated cargo sequestration into CCPs. TIRF microscopy images of Cos7 cells pretreated with DMSO or 30 μM pitstop 2 for 15 min were incubated with Alexa^{488}-EGF at 8°C in the continued presence of inhibitor and immunostained for AP-2α (red). Scale bar, 4 μm.

a minor decrease in the mean clathrin LC-eGFP intensity per object in TIRFM (Figure 4D). We noted a slightly increased dimming of CCPs in confocal when compared to TIRF imaging, presumably due to increased bleaching of stalled clathrin puncta. Thus, surprisingly, pitstop 2-mediated interference with clathrin TD-ligand association does not have a strong effect on the stability of membrane-associated clathrin, but dramatically perturbs CCP dynamics.

To corroborate the role of clathrin TD function in CCP dynamics fluorescence recovery after photobleaching (FRAP) was paired with live cell spinning disc confocal microscopy imaging. Following the bleaching laser pulse clathrin LC-eGFP fluorescence rapidly recovered to about 80% of its initial value with a τ of approximately 30 s in control cells, consistent with the mean CCP lifetimes measured by TIRFM-based particle tracking (compare Figures 4B and 4C). Pitstop 2-treated cells did not show recovery of clathrin LC-eGFP fluorescence within 120 s, confirming that clathrin TD function indeed regulates CCP dynamics. Recovery was so slow that a reliable τ value could not be determined under the imaging conditions. These data indicate that pitstop 2 stalls the maturation and/or consumption of pre-existing CCPs.

We next asked whether clathrin TD function may be required for the de novo assembly of clathrin-coated structures. We made use of 1-butanol, an alcohol which depletes cellular $PI(4,5)P_2$ levels causing CCP disassembly and loss of clathrin from the plasma membrane (Boucrot et al., 2006; Henne et al., 2010). Clathrin LC-eGFP containing pits rapidly reformed after washout of 1-butanol in control and pitstop 2-treated cells (Figure S3A). To corroborate that TD-ligand interactions are not required for the de novo clathrin recruitment, we re-expressed siRNA-resistant clathrin HC mutants in cells depleted of endogenous clathrin HC. Mutation of R64A/Q89M/F91A within the clathrin TD nearly abolished its ability to associate with amphiphysin to an extent similar to that seen for an amphiphysin mutant lacking its clathrin box (compare Figure 1F) but did not impair recruitment of full-length clathrin HC (R64A/Q89M/F91A) to the plasma membrane or to the TGN (Figure S3C). A clathrin HC mutant lacking the TD altogether (ΔTD) was also recruited to membranes (Figure S3C). We conclude that TD-ligand interactions are dispensable for clathrin recruitment to membranes.

If indeed pitstop 2 mainly interferes with CCP dynamics, one would expect relatively subtle effects on the distribution of endogenous endocytic proteins. Indeed, no significant changes were observed in the colocalization of clathrin, FCHo 1/2, intersectin, AP-2, or dynamin 2 (Figures S4A and S4B). We also did not detect overt changes with respect to the steady-state localization of HIP1, Dab2, GAK/auxilin2, or CALM (data not shown). This is not surprising as many endocytic proteins likely are retained at the plasma membrane by multiple interactions, i.e., by binding to AP-2 and/or membrane $PI(4,5)P_2$ as well as to each other (Schmid and McMahon, 2007).

Among the endocytic proteins analyzed, two clathrin accessory proteins displayed altered localizations. Endogenous amphiphysin 1 was partially lost from the plasma membrane of pitstop 2-treated cells (Figures S4C and S4D). Conversely, the mean intensity of SNX9-containing puncta was increased in pitstop 2-treated cells, often resulting in the formation of large clusters (Figures S3E–S3G). These findings correlate with the recent observation that amphiphysin and SNX9 operate at consecutive steps during CME (Taylor et al., 2011) and suggest that clathrin TD interactions may coordinate turnover of endocytic proteins at nascent CCPs.

We also determined the distribution of various TGN or endosomal proteins including AP-1, EEA1, Gadkin, CD63, TGN46, or the mannose 6-phosphate receptor MPR46. None of these factors showed a significant change in localization within 15 min of pitstop 2 application (Figures S5A and S5B). We did, however, note a partial shift of transferrin receptor (TfR) from perinuclear endosomes to the cell surface of pitstop 2-treated cells (Figure S4H), consistent with defective Tf endocytosis (Figures 3A and 3B).

Dynamics of FCHo2, AP-2, and Dynamin in Pitstop 2-Treated Cells

Since pitstop 2 impaired clathrin dynamics we next examined the behavior of other key endocytic proteins, which act either prior to or concomitant with clathrin assembly. FCHo proteins are early-acting factors that link $PI(4,5)P_2$-rich sites to AP-2 binding scaffolds such as intersectin and Eps15/Eps15R (Henne et al., 2010). TIRFM-based imaging of eGFP-FCHo2 dynamics in Cos7 cells revealed that FCHo2-containing structures were relatively long-lived, with lifetimes between 26 s and over 120 s. The mean lifetimes of FCHo2-eGFP-containing puncta were dramatically increased following application of pitstop 2 with puncta appearing nearly immobile (Figures 5A and 5B). Moreover, FCHo2-positive spots failed to recover in FRAP experiments (Figures 5C and 5D). Hence, clathrin TD function is required for the productive consumption of nascent CCPs containing FCHo2. Consistent with this and with the observation that pitstop 2 displaces the $PI(4,5)P_2$-consuming 5-phosphatases OCRL and synaptojanin 1-p170 from the clathrin TD (Figure 1E) pitstop 2 treatment also stabilized clathrin coats on membranes in vitro (Figures S3D and S3E).

Surprisingly, pitstop 2 induced a comparatively minor shift in the mean life span of AP-2σ-eGFP puncta (Figures 5E and 5F).

(E) Pearson's correlation between $Alexa^{488}$-EGF and AP-2. Data represent SEM (n = 3 independent experiments; *$p < 0.05$).
(F) Pitstop 2 does not affect clathrin-independent endocytosis of Shiga toxin. HeLa cells pretreated with DMSO or 30 μM pitstop 2 stained for internalizing Shiga toxin (red) and the *cis*-Golgi marker GM130 (green). Scale bar, 10 μm.
(G and H) Quantitative analysis of total and Golgi localized fractions of internalized Shiga toxin after 30 min of internalization. (SEM; differences are insignificant). Scale bar, 10 μm.
(I–J) Pitstop 2 blocks HIV infection. (I) Shown is the HIV Tat-driven luciferase activity in cells treated with increasing concentrations of pitstop 2 during infection. HIV Tat-driven luciferase activity in mock-treated cells was set as 100% infection. (J) Cytosolic entry of HIV-1-associated β-lactamase activity. Shown are ratiometric measurements (CCF-blue/CCF-green) of substrate cleavage by β-lactamase in cells treated with increasing concentrations of pitstop 2 during infection. See also Figure S3.

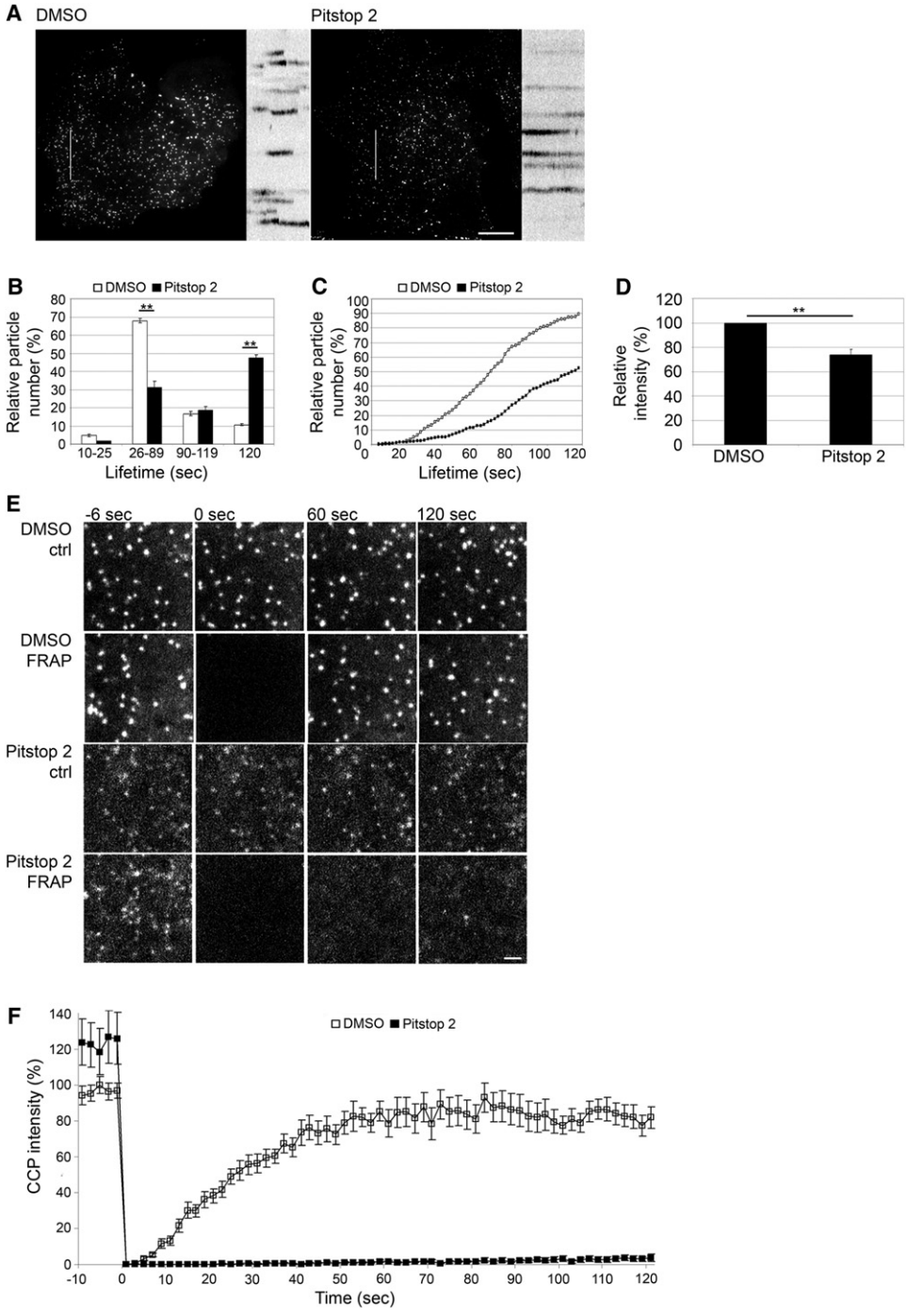

Figure 4. Pitstop 2 Affects the Dynamics of Clathrin-Coated Pits

Effects of pitstop 2 on clathrin dynamics were analyzed by live-cell TIRF or spinning disc confocal microscopy in Cos7 cells stably expressing eGFP-clathrin LC at 37°C.

(A) View of the clathrin distribution at the bottom surface of a cell pretreated for 5 min with 0.1% DMSO or 30 μM pitstop 2. Kymographs (right) display the dynamics of clathrin during the time-lapse series (2 min, 0.5 Hz). Scale bar, 10 μm.

(B) Pooled lifetime distribution of CCPs depicted in (A). Values were determined from the time between the appearance and disappearance of clathrin puncta (SEM; n = 2 independent experiments; **p < 0.01).

(C) Cumulative plot of clathrin lifetime distributions.

(D) Intensity of clathrin puncta in pitstop 2-treated cells. Mean fluorescence intensities of clathrin puncta in living cells were measured following addition of 0.1% DMSO or 30 μM pitstop 2 (SEM; n = 3 independent experiments; **p < 0.01).

These results are consistent with our observation that pitstop 2-treated cells remain able to sequester cargo into CCPs, a process largely mediated by AP-2 (compare Figures 3D and 3E).

Finally, we investigated the life span of the fissioning enzyme dynamin 2. Dynamin 2-eGFP displayed a lifetime distribution similar to that observed for AP-2 or clathrin. Pitstop 2 shifted this distribution to longer life spans with a behavior intermediary between the effects seen for clathrin and AP-2 (Figures 5G and 5H). Prolonged lifetimes of dynamin puncta at CCPs also fit well with the altered distribution of the dynamin-binding clathrin accessory proteins amphiphysin and SNX9 observed in pitstop-treated cells (Figures S3C–S3G).

Morphological Analysis of Pitstop 2-Treated Cells

Our live imaging data collectively argue that pitstop 2-mediated inhibition of CME results from defects in endocytic protein dynamics. As CME is a constitutive process in nonneuronal cells with CCPs forming and disassembling continuously, one would expect that acute perturbation of endocytic protein dynamics by pitstop 2-mediated inhibition of clathrin TD function results in acute ''trapping'' of clathrin-coated intermediates representing multiple stages of the pathway. To this aim, control or pitstop 2-treated Cos7 cells were subjected to electron microscopic and morphometric analyses. Clathrin-coated endocytic intermediates were classified according to their morphological profiles as shallow CCPs, nonconstricted u-shaped CCPs, constricted Ω-shaped CCPs corresponding to late fission stages, and structures containing a complete clathrin coat (Figure 6A). These latter intermediates may comprise free clathrin-coated vesicles as well as late intermediates that remain attached to the plasma membrane. Endocytic profiles of control cells and those incubated with pitstop 2 appeared very similar. No major changes in the total number of CCPs (Figure 6B) or in the representation of various endocytic stages were observed (Figure 6C). We conclude that pitstop-mediated inhibition of clathrin TD function acutely arrests CME at multiple stages.

Pitstops Inhibit Endocytic Recycling of Synaptic Vesicles in Neurons and In Situ

One of the most prominent functions of CME in vertebrates is the exo-endocytic recycling of synaptic vesicle (SV) membranes at nerve terminals (Dittman and Ryan, 2009). Unlike CME in nonneuronal cells endocytic reformation of SVs in neurons is strictly coupled to stimulation-dependent exocytosis resulting in a wave of endocytic activity (Dittman and Ryan, 2009). We tested the effects of pitstop 2-mediated clathrin inhibition on SV reformation in primary hippocampal neurons. Chemical stimulation of SV exocytosis resulted in a pronounced depletion of SVs from nerve terminals of pitstop 2-treated neurons, suggesting that SV reformation by endocytosis was inhibited. No significant changes in SV numbers were seen in resting control neurons (Figures S6A–S6C). Loss of SV membranes in pitstop 2-treated neurons appeared to be counterbalanced partly by presynaptic membrane expansion (Figure S6D).

The poor membrane penetration of pitstop 1 prevented analysis of its effects on endocytosis in living cells. However, its high solubility in aqueous media provided ideal conditions for its intracellular application by microinjection. We therefore assessed the effect of pitstops 1 and 2 on SV endocytosis in the lamprey reticulospinal synapse (Pechstein et al., 2010). We microinjected pitstop 1 into lamprey reticulospinal axons and stimulated at 5 Hz for 20 min to induce SV recycling at a physiological rate. Analysis of ultrathin sections revealed a profound loss of SVs at active zones in synapses from these axons (Figures 7A, 7B, and 7G), compared to control noninjected axons (Figure 7C). No morphological alterations were observed in axons microinjected with pitstop 1 and kept at rest (Figure 7E). Loss of SVs in stimulated axons was accompanied by a dramatic expansion of the plasma membrane, which due to anatomical constraints formed membrane pockets around the active zone (Figures 7A, 7B, and 7H). A significant accumulation of CCPs was observed within the membrane expansions compared with control synapses (Figures 7A–7C and 7I). Consistent with our observations in Cos7 cells, no dramatic alterations in stage representation of CCPs were observed (Figure 7J). No detectable morphological differences of CCPs were detected at high-magnification (Figures 7D and 7E). A similar phenotype including a pronounced loss of SVs and accumulation of multistage CCPs was observed in pitstop 2-injected reticulospinal synapses (Figure S7). We conclude that intra-axonal application of pitstops strongly inhibits SV recycling in situ by inhibiting CME at multiple stages.

DISCUSSION

We have developed chemically distinct small molecule inhibitors of clathrin TD function termed pitstops that competitively interfere with the association of endocytic clathrin box ligands. In vitro experiments in conjunction with structural data based on protein X-ray crystallography as well as experiments in living cells clearly demonstrated that these compounds selectively perturb clathrin TD function. Effects of pitstop 2 on CME are evident within a few minutes of cell treatment, presumably only being limited by the rate of drug diffusion across the cell membrane. We observe reversible inhibition of CME in a broad variety of cells at concentrations closely matching the IC_{50} values of the in vitro binding experiments. While pitstop 2 readily crosses cell membranes, pitstop 1 has greatly reduced efficacy, limiting its use to live cell applications based on intracellular application. The similarity of phenotypes exhibited by pitstops 1 and 2 in lamprey reticulospinal synapses in situ and in Cos 7 cells in vitro suggests that both compounds share a common

(E) Pitstop 2 stalls clathrin dynamics. Fluorescence recovery after photobleaching (FRAP) of clathrin LC-labeled CCPs in an area of 15 × 15 μm^2. Cells were imaged 5 min after the addition of 30 μM pitstop 2 or DMSO (0.1%) using spinning disc confocal microscopy. Frames were taken at 0.5 Hz, starting 10 s before FRAP, followed by imaging for another 2 min after photobleaching. The panels represent images of the FRAP region and an unbleached control area in DMSO- or pitstop 2-treated cells acquired before (−6 s), right after (0 s), 1 min, and 2 min after photobleaching. Scale bar, 2 μm.

(F) Corrected relative fluorescence intensities of clathrin puncta in the FRAP region over time (SEM; n = 2 independent experiments; $^{**}p < 0.01$).

See also Figure S4.

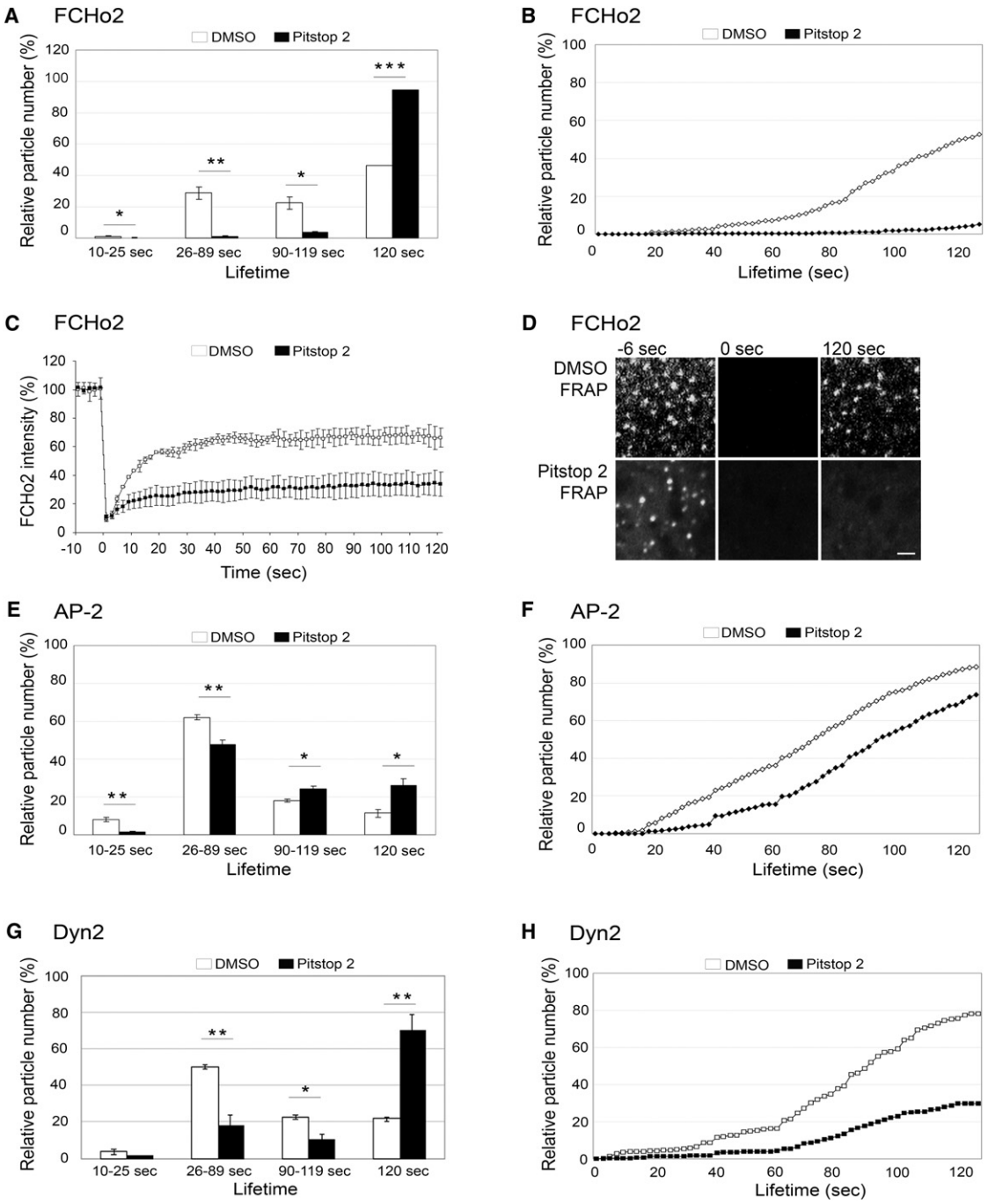

Figure 5. Differential Effects of Pitstop 2 on the Dynamics of FCHo2, AP-2, and Dynamin

Effects of pitstop 2 on endocytic protein dynamics were analyzed by live-cell TIRF or spinning disc confocal microscopy in Cos7 cells transiently expressing low levels of eGFP-tagged FCHo2, AP-2σ, or dynamin 2.

(A, E, and G) Pooled lifetime distributions of eGFP-FCHo2 (A), AP-2σ-eGFP (E), and Dyn2-eGFP (G) puncta in cells pretreated for 5 min with 0.1% DMSO or 30 μM pitstop 2. Plots represent the time between the appearance and disappearance of the fusion protein-containing puncta in a time lapse-series acquired for 2 min at 0.5 Hz (SEM; n = 2 independent experiments; *p < 0.05, **p < 0.01, ***p < 0.001).

(C) Effect of pitstop 2 on FRAP of FCHo2-containing puncta in an area of 15 × 15 μm^2. Samples were analyzed as described in the legend to Figure 4E (SEM; n = 2 independent experiments).

(D) Images of the FRAP region in DMSO- or pitstop 2-treated cells acquired before (−6 s), right after (0 s), and 2 min after photobleaching. Scale bar, 2 μm.

(B, F, and H) Cumulative plots of the lifetime distributions of FCHo2 (B), AP-2 (F), and Dynamin 2 (H).

See also Figure S5.

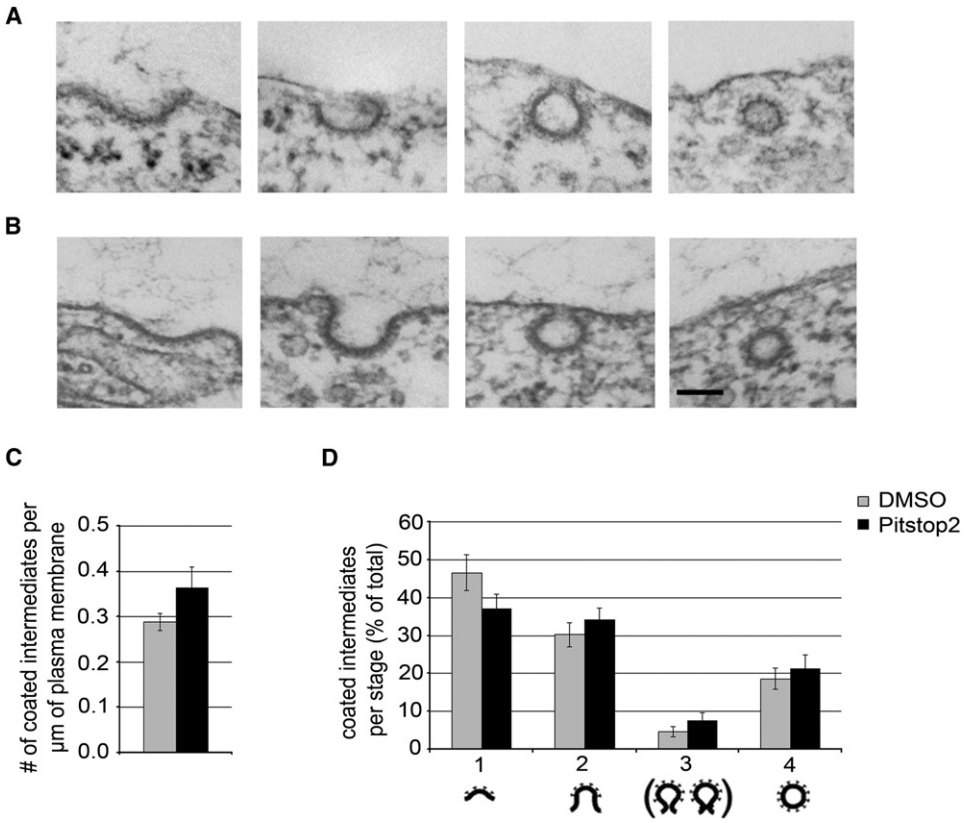

Figure 6. Ultrastructural Analysis of Intermediates Observed in Pitstop 2-Treated Cells

(A and B) Representative examples of clathrin-coated structures observed at the plasma membrane of Cos7 cells pretreated for 5 min with 0.1% DMSO (A) or 30 μM pitstop 2 (B). Scale bar, 200 nm. Morphological groups were shallow CCPs (stage 1), nonconstricted u-shaped CCPs (stage 2), constricted Ω-shaped CCPs (stage 3), or structures containing complete clathrin coats (stage 4).

(C) Bar diagram displaying the numbers of clathrin-coated endocytic intermediates observed along the perimeter of Cos7 cells treated with 0.1% DMSO or 30 μM pitstop 2.

(D) Bar diagram showing the relative abundance of different stages of coated endocytic intermediates observed along the perimeter of Cos7 cells treated with 0.1% DMSO or 30 μM pitstop 2.

See also Figure S6.

clathrin TD-based molecular mechanism of action. In the presence of pitstop 2 clathrin-independent internalization pathways and secretory traffic (data not shown) remain unperturbed. Therefore, pitstops represent new cellular tools to selectively inhibit CME.

Pitstops Block CME by Interfering with CCP Dynamics

The use of pitstops in living cells revealed an unexpected role for the clathrin TD and its ligands in endocytic pit dynamics while clathrin recruitment was unperturbed. Together with the observation that clathrin lacking its TD is targeted to CCPs, it is likely that other interactions such as the association of the β-ear domain of AP-2 with the clathrin leg (Knuehl et al., 2006) mediate clathrin recruitment to membranes.

Our data are explained by a model where pitstops interfere with the progression of CCPs at multiple stages, consistent with the functional diversity of clathrin TD ligands. Clathrin is one of a few molecules within the endocytic network with the ability to spatiotemporally regulate vesicle formation and disassembly after fission. Most endocytic proteins partially lack stable tertiary structure or contain extensive segments of natively unfolded polypeptide chains, but clathrin triskelia are stable entities with a fixed arrangement, distance, and geometry between their TDs (Brodsky et al., 2001). We, thus, favor a model whereby clathrin assembled at nascent endocytic sites serves as an organizing scaffold that regulates CCP dynamics by providing spatially defined binding sites on its TD for accessory proteins that drive CCP maturation and disassembly (Figure 1A, right). The specific mechanisms that regulate such transitions within an assembling or disassembling CCP are unknown, but pitstops together with dynamin inhibitors (Joshi et al., 2010; Macia et al., 2006) may provide powerful tools to tackle these questions.

Unraveling the Roles of Clathrin in Cell Physiology

Evidence from morphological, genetic, and knockdown studies has suggested that CME may be a key mechanism for SV recycling (Dittman and Ryan, 2009). The fact that synapses can adapt to chronic loss of endocytic proteins is a substantial drawback for RNAi and genetic approaches. Our data using pitstops provide a direct demonstration for an important role of clathrin

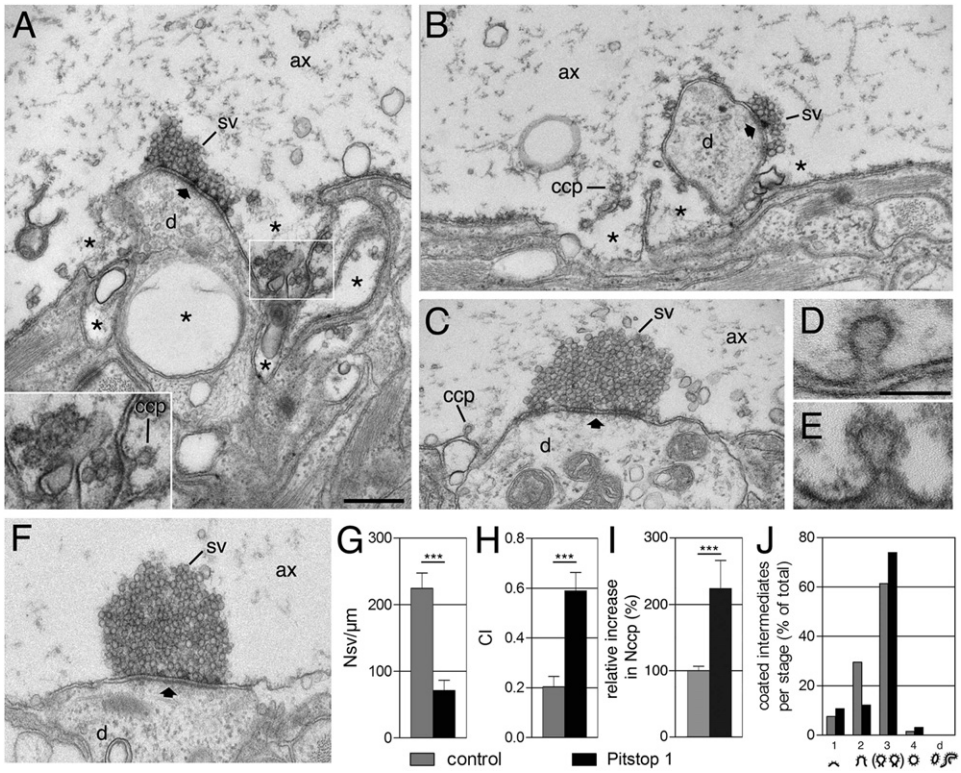

Figure 7. Pitstop 1 Inhibits Activity-Induced SV Recycling in Lamprey Reticulospinal Synapses

(A and B) Electron micrographs of reticulospinal synapses microinjected with pitstop 1 and stimulated at 5 Hz for 20 min. SVs (sv) are depleted from sites of release. Instead, large membrane expansions and pockets (asterisks) are seen, which in some sections (e.g., in B) surrounded the active zone (marked with thick arrows). Boxed area containing clathrin-coated pits (CCPs) is shown as inset at higher magnification in (A).

(C) EM image of a control noninjected synapse from the same spinal cord preparation.

(D and E) Constricted CCPs from a control noninjected axon and a synapse microinjected with pitstop 1. Note the similar shape of CCPs and the presence of clathrin coats in both cases.

(F) Electron micrograph of a synapse microinjected with pitstop 1 but kept at rest.

(G–I) Bar diagrams displaying numbers of SVs (Nsv), curvature index (CI), and the number of clathrin-coated intermediates (Nccp) between control synapses stimulated at 5 Hz (gray bars) and pitstop 1-microinjected stimulated synapses (black bars), respectively. ax, axoplasmic matrix; d, dendrite.

(J) Bar diagram showing the relative abundance of different stages of coated endocytic intermediates (see legend to Figure 6A) in control synapses stimulated at 5 Hz (gray bars) and stimulated synapses microinjected with pitstop 1 (black bars).

Scale bars for (A–C) and (F), 0.5 µm and for (D) and (E), 100 nm.

See also Figure S7.

in SV recycling in vertebrate neurons under conditions of high activity. The development of pitstops will allow further molecular dissection of clathrin function under different stimulation paradigms and in different preparations.

Our data also lend strong support to the hypothesis that HIV enters cells largely via CME (Daecke et al., 2005; Miyauchi et al., 2009). Hence, we predict that the inhibitors developed here or derivatives thereof may serve as lead compounds for the development of drugs blocking the entry of viruses and pathogens, which hijack the clathrin machinery, including HIV, hepatitis C virus (Blanchard et al., 2006), ebola virus (Bhattacharyya et al., 2010), and *Listeria monocytogenes* (Veiga et al., 2007).

It is to be expected that acute interference with clathrin TD function will affect other clathrin-dependent pathways. Clathrin plays roles in bidirectional traffic between the *trans*-Golgi network and endosomes, a pathway mediated by AP-1 and GGA adaptors (Bonifacino and Traub, 2003; Hirst et al., 2009). Clathrin coats have also been observed on endosomes, where clathrin may fulfill a structural role in the segregation of endosomal membrane domains involved in targeting of growth factor receptors (Goh et al., 2010) to the multivesicular body pathway or in directing retrograde transport (Saint-Pol et al., 2004). Finally, clathrin has been detected at the mitotic spindle where it has been proposed to stabilize microtubules (Royle et al., 2005). Whether and to which degree these functions depend on the association of conventional clathrin box ligands with the TD can now be addressed using the small molecule inhibitor approach.

Pitstops will serve as an important tool to address these questions as well as more generally the role of clathrin function in cell physiology including cell signaling. The availability of crystal structures of pitstops in complex with the clathrin TD will pave the way for the development of second- and third-generation compounds with increased affinity and improved molecular properties that could serve as prodrugs for the treatment of

multiple diseases ranging from neurological disorders to microbial infections.

EXPERIMENTAL PROCEDURES

Information regarding compound synthesis, antibodies, DNA constructs, cell viability assays, protein purification, crystallography, fluorescence microscopy, Shiga toxin uptake, and HIV infection are available as supplementary material online.

Screening Procedure

Seventeen thousand small molecules (100 μM) from the central open access technology platform of the ChemBioNet hosted by FMP (http://fmp-berlin.info/screening_unit.html) were screened using an automated platform for their ability to perturb clathrin TD-amphiphysin association using an ELISA-based assay in a 384-well format (see below for details). Forty-eight initial hits (>80% inhibition) were selected. Ten of these hits could be validated by dose-response analysis (at 3–300 μM) and structural hit clustering. Hits were verified using compounds re-ordered from the ChemDiv collection. Two lead compounds were selected based on the absence of off-target effects and inhibition of transferrin endocytosis. Focused libraries synthesized based on these leads were re-screened as above resulting in the identification of pitstops 1 and 2. Pitstop, pitstop 1, and pitstop 2, are trademarks of Freie Universität Berlin, Children's Medical Research Institute and Newcastle Innovation Ltd. Pitstop 1 and pitstop 2 are available from Ascent Scientific Ltd.

ELISA-Based Binding Assay

Purified His_6-tagged protein was diluted into screening buffer (20 mM HEPES [pH 7.4], 50 mM NaCl, 1 mM DTT, 1 mM PMSF), added to a 384-well ELISA plate (high-binding PS Microplate, Greiner Bio-One) and bound for 1 hr at RT. Nonspecific binding was blocked by incubation in 50 μl blocking buffer (20 mM HEPES [pH 7.4], 50 mM NaCl, 1 mM DTT, 1 mM PMSF, 2% BSA, 2.5% milk) overnight at 4°C. Following extensive washes with 20 mM HEPES (pH 7.4), 50 mM NaCl, 0.05% Tween 20, chemical compounds diluted in DMSO (10 μl) were added and incubated together with GST-tagged protein for 1 hr at RT in screening buffer. After three washes, HRP-coupled anti-GST antibodies were added in screening buffer and the plate was incubated for 15 min at RT. Following additional washes, bound protein was determined by photometric measurement in a plate reader at 450 nm using TMB as a substrate (Pierce Biotechnology).

Confocal and TIRF-Based Live Imaging

For live cell microscopy Cos7 cells stably expressing eGFP-clathrin LC (Gaidarov et al., 1999), or transiently expressing FCHo2-eGFP, AP-2σ-eGFP (Gaidarov et al., 1999), and dynamin2-eGFP were used. CCP dynamics were imaged by TIRFM (Visitron) under the control of Slidebook 5 (3i Inc). Time series of 2 min (at 0.5 Hz) were acquired 5 min after addition of 30 μM pitstop 2 or DMSO (0.1%) at 37°C. Fluorescence recovery after photobleaching (FRAP) experiments were performed using a spinning disc confocal microscope (Perkin Elmer) controlled by Volocity (Improvision). Time series were acquired 5 min after addition of 30 μM pitstop 2 or DMSO (0.1%) at 37°C. Cells were imaged for 12 s, then bleached in a region of 15 × 15 μm^2, and imaged for an additional 120 s at 0.5 Hz. Fluorescence recovery was analyzed by defining CCPs in the FRAP region before bleaching, followed by measuring the fluorescence intensity in the FRAP region over time. Intensity values were corrected for photobleaching in a nonbleached control area.

Electron Microscopy

Electron microscopic analyses were essentially done as described in Ferguson et al. (2009). See Extended Experimental Procedures for details.

Microinjection of Compounds into Lamprey Reticulospinal Axons and Analysis by Electron Microscopy

Microinjection experiments and electron microscopic analysis were essentially done as previously described (Pechstein et al., 2010). See supplement for details.

ACCESSION NUMBERS

Structures are accessible under PDB codes 2xzg and 2xzh.

SUPPLEMENTAL INFORMATION

Supplemental Information includes Extended Experimental Procedures, two tables, and seven figures and can be found with this article online at doi:10.1016/j.cell.2011.06.025.

ACKNOWLEDGMENTS

We thank Drs. Gilbert Di Paolo, Ludger Johannes, and Oliver Daumke for critical comments and Drs. Harvey Mc Mahon, Ludger Johannes, Pietro De Camilli, Tom Sudhof, and Sven Carlsson for reagents. Cytotoxicity assays were conducted with help from Aimee Novelle, Swetha Perera, and Dr. Jayne Gilbert. This work was supported by grants from the Deutsche Forschungsgemeinschaft (FOR 806-HA2686/3-1,3-2; SFB765/B4 to V.H.; Exc-257), the European Science Foundation (Euromembrane-HA2686/6-1), and the Swedish Research Council (grants 13473 and 20587 to O.S.).

Received: December 21, 2010
Revised: May 6, 2011
Accepted: June 14, 2011
Published: August 4, 2011

REFERENCES

Bhattacharyya, S., Warfield, K.L., Ruthel, G., Bavari, S., Aman, M.J., and Hope, T.J. (2010). Ebola virus uses clathrin-mediated endocytosis as an entry pathway. Virology *401*, 18–28.

Blanchard, E., Belouzard, S., Goueslain, L., Wakita, T., Dubuisson, J., Wychowski, C., and Rouille, Y. (2006). Hepatitis C virus entry depends on clathrin-mediated endocytosis. J. Virol. *80*, 6964–6972.

Bonifacino, J.S., and Traub, L.M. (2003). Signals for sorting of transmembrane proteins to endosomes and lysosomes. Annu. Rev. Biochem. *72*, 395–447.

Boucrot, E., Saffarian, S., Massol, R., Kirchhausen, T., and Ehrlich, M. (2006). Role of lipids and actin in the formation of clathrin-coated pits. Exp. Cell Res. *312*, 4036–4048.

Brodsky, F.M., Chen, C.Y., Knuehl, C., Towler, M.C., and Wakeham, D.E. (2001). Biological basket weaving: formation and function of clathrin-coated vesicles. Annu. Rev. Cell Dev. Biol. *17*, 517–568.

Conner, S.D., and Schmid, S.L. (2003). Regulated portals of entry into the cell. Nature *422*, 37–44.

Daecke, J., Fackler, O.T., Dittmar, M.T., and Kräusslich, H.G. (2005). Involvement of clathrin-mediated endocytosis in human immunodeficiency virus type 1 entry. J. Virol. *79*, 1581–1594.

Dittman, J., and Ryan, T.A. (2009). Molecular circuitry of endocytosis at nerve terminals. Annu. Rev. Cell Dev. Biol. *25*, 133–160.

Edeling, M.A., Smith, C., and Owen, D. (2006). Life of a clathrin coat: insights from clathrin and AP structures. Nat. Rev. Mol. Cell Biol. *7*, 32–44.

Ehrlich, M., Boll, W., Van Oijen, A., Hariharan, R., Chandran, K., Nibert, M.L., and Kirchhausen, T. (2004). Endocytosis by random initiation and stabilization of clathrin-coated pits. Cell *118*, 591–605.

Ferguson, S.M., Raimondi, A., Paradise, S., Shen, H., Mesaki, K., Ferguson, A., Destaing, O., Ko, G., Takasaki, J., Cremona, O., et al. (2009). Coordinated actions of actin and BAR proteins upstream of dynamin at endocytic clathrin-coated pits. Dev. Cell *17*, 811–822.

Gaidarov, I., Santini, F., Warren, R.A., and Keen, J.H. (1999). Spatial control of coated-pit dynamics in living cells. Nat. Cell Biol. *1*, 1–7.

Goh, L.K., Huang, F., Kim, W., Gygi, S., and Sorkin, A. (2010). Multiple mechanisms collectively regulate clathrin-mediated endocytosis of the epidermal growth factor receptor. J. Cell Biol. *189*, 871–883.

Heerssen, H., Fetter, R.D., and Davis, G.W. (2008). Clathrin dependence of synaptic-vesicle formation at the Drosophila neuromuscular junction. Curr. Biol. *18*, 401–409.

Henne, W.M., Boucrot, E., Meinecke, M., Evergren, E., Vallis, Y., Mittal, R., and McMahon, H.T. (2010). FCHo proteins are nucleators of clathrin-mediated endocytosis. Science *328*, 1281–1284.

Hinrichsen, L., Meyerholz, A., Groos, S., and Ungewickell, E.J. (2006). Bending a membrane: how clathrin affects budding. Proc. Natl. Acad. Sci. USA *103*, 8715–8720.

Hirst, J., Sahlender, D.A., Choma, M., Sinka, R., Harbour, M.E., Parkinson, M., and Robinson, M.S. (2009). Spatial and functional relationship of GGAs and AP-1 in Drosophila and HeLa cells. Traffic *10*, 1696–1710.

Johannes, L., and Römer, W. (2010). Shiga toxins—from cell biology to biomedical applications. Nat. Rev. Microbiol. *8*, 105–116.

Joshi, S., Perera, S., Gilbert, J., Smith, C.M., Mariana, A., Gordon, C.P., Sakoff, J.A., McCluskey, A., Robinson, P.J., Braithwaite, A.W., and Chircop, M. (2010). The dynamin inhibitors MiTMAB and OcTMAB induce cytokinesis failure and inhibit cell proliferation in human cancer cells. Mol. Cancer Ther. *9*, 1995–2006.

Knuehl, C., Chen, C.Y., Manalo, V., Hwang, P.K., Ota, N., and Brodsky, F.M. (2006). Novel binding sites on clathrin and adaptors regulate distinct aspects of coat assembly. Traffic *7*, 1688–1700.

Macia, E., Ehrlich, M., Massol, R., Boucrot, E., Brunner, C., and Kirchhausen, T. (2006). Dynasore, a cell-permeable inhibitor of dynamin. Dev. Cell *10*, 839–850.

Mettlen, M., Stoeber, M., Loerke, D., Antonescu, C.N., Danuser, G., and Schmid, S.L. (2009). Endocytic accessory proteins are functionally distinguished by their differential effects on the maturation of clathrin-coated pits. Mol. Biol. Cell *20*, 3251–3260.

Miyauchi, K., Kim, Y., Latinovic, O., Morozov, V., and Melikyan, G.B. (2009). HIV enters cells via endocytosis and dynamin-dependent fusion with endosomes. Cell *137*, 433–444.

Motley, A., Bright, N.A., Seaman, M.N., and Robinson, M.S. (2003). Clathrin-mediated endocytosis in AP-2-depleted cells. J. Cell Biol. *162*, 909–918.

Pechstein, A., Bacetic, J., Vahedi-Faridi, A., Gromova, K., Sundborger, A., Tomlin, N., Krainer, G., Vorontsova, O., Schäfer, J.G., Owe, S.G., et al. (2010). Regulation of synaptic vesicle recycling by complex formation between intersectin 1 and the clathrin adaptor complex AP2. Proc. Natl. Acad. Sci. USA *107*, 4206–4211.

Royle, S.J., Bright, N.A., and Lagnado, L. (2005). Clathrin is required for the function of the mitotic spindle. Nature *434*, 1152–1157.

Saffarian, S., Cocucci, E., and Kirchhausen, T. (2009). Distinct dynamics of endocytic clathrin-coated pits and coated plaques. PLoS Biol. *7*, e1000191.

Saint-Pol, A., Yélamos, B., Amessou, M., Mills, I.G., Dugast, M., Tenza, D., Schu, P., Antony, C., McMahon, H.T., Lamaze, C., and Johannes, L. (2004). Clathrin adaptor epsinR is required for retrograde sorting on early endosomal membranes. Dev. Cell *6*, 525–538.

Schmid, E.M., and McMahon, H.T. (2007). Integrating molecular and network biology to decode endocytosis. Nature *448*, 883–888.

Slepnev, V.I., Ochoa, G.C., Butler, M.H., and De Camilli, P. (2000). Tandem arrangement of the clathrin and AP-2 binding domains in amphiphysin 1 and disruption of clathrin coat function by amphiphysin fragments comprising these sites. J. Biol. Chem. *275*, 17583–17589.

Taylor, M.J., Perrais, D., and Merrifield, C.J. (2011). A high precision survey of the molecular dynamics of mammalian clathrin-mediated endocytosis. PLoS Biol. *9*, e1000604.

ter Haar, E., Harrison, S.C., and Kirchhausen, T. (2000). Peptide-in-groove interactions link target proteins to the beta-propeller of clathrin. Proc. Natl. Acad. Sci. USA *97*, 1096–1100.

Veiga, E., Guttman, J.A., Bonazzi, M., Boucrot, E., Toledo-Arana, A., Lin, A.E., Enninga, J., Pizarro-Cerdá, J., Finlay, B.B., Kirchhausen, T., and Cossart, P. (2007). Invasive and adherent bacterial pathogens co-Opt host clathrin for infection. Cell Host Microbe *2*, 340–351.